Cell, Vol. 103, 885–896, December 8, 2000, Copyright ©2000 by Cell Press

Crystal Structure of a β-Catenin/Tcf Complex

Thomas A. Graham,*† Carole Weaver,‡§ Feng Mao,* David Kimelman,‡ and Wenqing Xu*‖

*Department of Biological Structure
†Biomolecular Structure and Design Program
‡Department of Biochemistry
§Molecular and Cellular Biology Program
University of Washington
Seattle, Washington 98195

Summary

The Wnt signaling pathway plays critical roles in embryonic development and tumorigenesis. Stimulation of the Wnt pathway results in the accumulation of a nuclear β-catenin/Tcf complex, activating Wnt target genes. A crystal structure of β-catenin bound to the β-catenin binding domain of Tcf3 (Tcf3-CBD) has been determined. The Tcf3-CBD forms an elongated structure with three binding modules that runs antiparallel to β-catenin along the positively charged groove formed by the armadillo repeats. Structure-based mutagenesis defines three sites in β-catenin that are critical for binding the Tcf3-CBD and are differentially involved in binding APC, cadherin, and Axin. The structural and mutagenesis data reveal a potential target for molecular drug design studies.

Introduction

β-catenin is critically required for cell adhesion and as an intracellular mediator of the Wnt pathway. The great majority of β-catenin is found at the cell membrane where it mediates cadherin-based cell adhesion through interactions with the cytoplasmic region of cadherin and α-catenin (reviewed by Provost and Rimm, 1999). A smaller pool of β-catenin in the nucleus and cytoplasm is regulated by Wnt signals. In unstimulated cells, cytosolic β-catenin is constitutively degraded by a ubiquitin ligase-proteosome system. Wnt signaling inhibits this process, allowing β-catenin to accumulate and subsequently translocate to the nucleus where it forms a transcriptional activating complex with members of the Tcf/LEF-1 family of proteins. Genetic and biochemical studies have demonstrated that the Wnt signaling pathway controls many processes in embryonic development in both vertebrates and invertebrates (reviewed by Moon and Kimelman, 1998; Wodarz and Nusse, 1998; Peifer and Polakis, 2000). Moreover, inappropriate activation of the Wnt intracellular pathway is associated with various human cancers, in particular colon cancer (reviewed by Kinzler and Vogelstein, 1996; Morin, 1999; Polakis, 2000). For both embryonic development and tumorigenesis, formation of the complex between β-catenin and Tcf is the critical step in the activation of Wnt target genes (reviewed by Bienz and Clevers, 2000).

How the Wnt signaling pathway controls the protein level of β-catenin continues to be an area of intensive study. In the current view, phosphorylation of β-catenin by GSK-3β (glycogen synthase kinase-3β) regulates the turnover of β-catenin (reviewed by Peifer and Polakis, 2000; Seidensticker and Behrens, 2000). In the absence of a Wnt signal, a cytoplasmic protein complex called the "β-catenin destruction complex," containing GSK-3β, the APC (adenomatous polyposis coli) protein, and the scaffolding protein Axin, catalyzes the phosphorylation of β-catenin. A ubiquitin ligase complex recognizes phosphorylated β-catenin and targets it for degradation by the proteosome. Active Wnt signaling inhibits the phosphorylation of β-catenin by GSK-3β by a mostly unknown mechanism, thus preventing the degradation of β-catenin.

Tcf/LEF-1 family members, Axin, APC, and the cadherins bind β-catenin in the large central core of the protein, which contains 12 armadillo repeats. The previously reported crystal structure of the armadillo repeat region of murine β-catenin revealed that each repeat consists of three α helices, and together the 12 repeats form a superhelix that features a long positively charged groove (Huber et al., 1997). While the β-catenin binding domain (CBD) of the different β-catenin partners has been well defined in several cases (Hulsken et al., 1994; Rubinfeld et al., 1995; Behrens et al., 1996; Molenaar et al., 1996; Orsulic and Peifer, 1996; Pai et al., 1996; Ikeda et al., 1998), there has been no obvious homology found among them. No previous three-dimensional structural information is available for any of the CBDs. However, the well-studied CBDs are highly negatively charged under physiological pH, and phosphorylation of APC and cadherin CBDs enhances their β-catenin binding activity. It has thus been proposed that the positively charged groove of β-catenin may be important for interacting with the negatively charged CBDs (Huber et al., 1997).

The CBD of Tcf/LEF-1 family members corresponds to approximately 60 amino acids at the very N terminus of the protein (Behrens et al., 1996; Molenaar et al., 1996; Korinek et al., 1997; van de Wetering et al., 1997). Two conserved residues in Tcf4-CBD, Asp-16 and Leu-48, have been defined by mutagenesis as critical residues for the interaction of Tcf4 with β-catenin (Omer et al., 1999). All Tcf/LEF-1 family members also have a highly conserved HMG DNA binding domain, located within the C-terminal half of the protein. Tcf/LEF-1 proteins by themselves have no innate transcriptional activity and they repress transcription of Wnt target genes by recruiting corepressors to the promoter (reviewed by Roose and Clevers, 1999; Barker et al., 2000). Transcriptional activation of target genes occurs when β-catenin binds the Tcf/LEF-1 factors and recruits transcription factors, such as p300/CBP and the TATA binding protein, to the promoter (Hecht et al., 1999, 2000; Kato et al., 1999; Takemaru and Moon, 2000).

Deletion analysis of the β-catenin armadillo repeats

‖To whom correspondence should be addressed (e-mail: wxu@u.washington.edu).

has not resolved whether its partners bind to discrete spots on β-catenin using their divergent CBDs, or whether they bind via a few key shared sites. This question becomes important since compounds that block the interaction between β-catenin and Tcf could be useful pharmacological agents for the treatment of cancers that result from inappropriate activation of the Wnt pathway. However, it is critical that these compounds do not interfere with β-catenin/cadherin interactions, which would result in widespread alterations in cell adhesion.

We now report the three-dimensional structure of a β-catenin/Tcf3-CBD complex, determined by X-ray crystallography at 2.1 Å resolution. This structure of a β-catenin partner bound to β-catenin has allowed us to define critical sites on β-catenin required for interacting with Tcf and other members of the Wnt pathway.

Results

Overall Structure

We used the armadillo repeat region of human β-catenin (residues 134–664) and the β-catenin binding domain of *Xenopus* Tcf3 (XTcf3-CBD, residues 1–61 of Xtcf3) in our crystallographic studies. There are only six residues that are different between the armadillo repeat regions of human and *Xenopus* β-catenins; all six are located on the β-catenin surface far from the groove that is predicted to be the protein–protein interaction site. In the crystal, one molecule of β-catenin interacts with one molecule of XTcf3-CBD, and there are two β-catenin/XTcf3-CBD complexes in each asymmetric unit (see Table 1). For convenience, we use "β-catenin" to refer to the armadillo repeat region of β-catenin in this work.

The β-catenin in the β-catenin/XTcf3-CBD complex has essentially the same structure as the previously reported unbound β-catenin. The rmsd of the Cα positions between unbound and bound β-catenin is 0.76 Å and 0.56 Å for the two β-catenin/XTcf3-CBD complexes in the asymmetric unit, respectively. The rmsd of comparable Cα positions of β-catenin in the two β-catenin/XTcf3-CBD complexes is 0.56 Å.

The XTcf3-CBD forms an elongated structure that runs antiparallel along the positively charged groove of β-catenin (Figure 1A). XTcf3-CBD can be roughly divided into three binding modules. From the N to C terminus, XTcf3-CBD contains a β hairpin module (residues 2–15), an extended region (residues 16–29), and an α helix (residues 40–51) (Figure 1B). Residues 30–39 and residues C-terminal to residue 51 of Tcf3-CBD are not well ordered and are therefore not included in our model. All three well-ordered modules form extensive contacts with β-catenin. The Tcf3-CBD β hairpin fits into the groove formed by armadillo repeats 9 and 10. Residues 16–29 travel in the groove as an extended strand in a direction that is roughly perpendicular to the third helices of armadillo repeats 5–8 of β-catenin (Figure 1A). In this region, residues 16–24 are in a β strand conformation. Residues 40–51 form an α helix and continue to travel along the groove, packing on the third helices of armadillo repeats 3 and 4.

Table 1. Structure Determination and Refinement

Data Collection Statistics	
Space group	$P2_12_12_1$
Unit cell dimensions (Å)	a = 52.14, b = 153.25, c = 188.124
No. of complexes per asymmetric unit	2
Resolution (Å)	25.0–2.1
Observed/unique reflections	300,150/82,185
Completeness (last shell) %	92.3 (94.8)
[1]R_{sym} (last shell) %	5.2 (30.4)
I/σ (last shell)	16.2 (4.0)
Refinement Statistics	
No. of reflections (working, test)	66,341/7,442
R_{work}/R_{free} (%)	22.9/25.5
rmsd from ideality	
Bond length (Å)	0.005
Bond angle (°)	1.04
Dihedral angle (°)	18.4
Ramachandran plot (core, disallowed) %	95.6/0.0
Average B factor (w/o solvent, w/ solvent)	38.3/38.8
rmsd of B factors (bonded atoms main chain/side chain)	0.89/1.42
No. of protein atoms in the final model	7,538
No. of H_2O molecules in the final model	263

[1]$R_{sym} = \Sigma_{ij}|I_i(j) - < I(j) > |/\Sigma_{ij}I_i(j)$, where $I_i(j)$ is the i-th measurement of reflection j and $< I(j) >$ is the overall weighted mean of j measurements.

Interactions between β-Catenin and the β Hairpin Module of XTcf3-CBD

The N terminus of XTcf3-CBD protrudes from the groove in β-catenin by interacting with residues in armadillo repeats 9 to 11 (Figure 2A). The surface area buried by the β hairpin is approximately 1760 Å^2. Residues 8–15 of XTcf3 form an antiparallel β hairpin, and fit into the deep groove caused by a kink around armadillo repeat 9 (Figure 2A). The lack of side chains in Gly-8 and Gly-9 of XTcf3 is required so that the strand composed of residues 8–11 may be buried deeper in the groove than the other strand of the β hairpin. The β hairpin is stabilized by extensive hydrogen bonding between XTcf3, β-catenin, and ordered water molecules (Figure 2B). Three arginine residues in β-catenin form contacts with the XTcf3 β hairpin module from three different directions. Arg-474 and Arg-612 form two salt bridges with the side chains of XTcf3-CBD Asp-10 and Glu-11, respectively. The third arginine residue, Arg-582, coordinates with Glu-11 of XTcf3-CBD as well (Figure 2B).

Interactions between β-Catenin and the Extended Region of XTcf3-CBD

The extended region of XTcf3-CBD consists of residues Asp-16 through Glu-29. The total surface area buried by this region is approximately 1860 Å^2. Residues 16 to 24 form a β strand that allows every side chain, as well

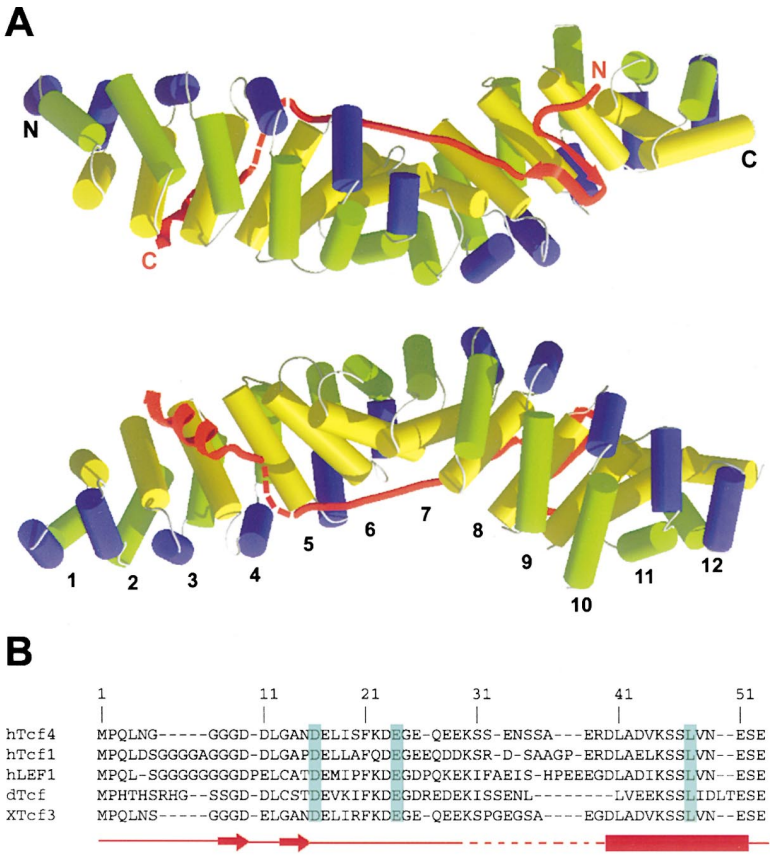

Figure 1. The Overall Structure of the XTcf3-CBD/β-Catenin Armadillo Complex

(A) Two views of the complex are related by a 180° rotation about the β-catenin superhelical axis. The armadillo repeat region of β-catenin forms a superhelix made of 12 repeats. Each repeat, except repeat 7, consists of three helices that are shown in blue, green, and yellow, respectively. XTcf3-CBD is shown in red and consists of, from N terminus to C terminus, a β hairpin module, an extended region that contains a β strand, and an α helix. Unresolvable residues are denoted by the dashed lines. XTcf3-CBD wraps around the armadillo repeat region of β-catenin in an antiparallel fashion along the major axes of the superhelix. Note that the path taken by the XTcf3-CBD follows the groove of the β-catenin armadillo repeat region. The surface of this groove is made up of the third helices of repeats 3–10 (in yellow). The figure was generated by MOLSCRIPT and RASTER3D (Kraulis, 1991; Merritt and Murphy, 1994).

(B) The sequence alignment of representative Tcf/LEF-1 family members. The topology of this region of XTcf3 is shown in red. The β strands are denoted by arrows and the helix is denoted by a box. The residues that play critical roles in the XTcf3-CBD/β-catenin interaction, as determined by mutagenesis studies, are marked in turquoise.

as main chain atoms, to contact β-catenin in the β-catenin groove (Figure 3). One key feature of this region of β-catenin is the two semi-buried lysine residues (Lys-312 and Lys-435) that bind to either end of the β strand in the extended region of XTcf3-CBD (Figure 3B). The δ-amino group of β-catenin Lys-435 sits in the bottom of a deep valley and coordinates with the carboxyl side chain of Asp-16 of the XTcf3-CBD. Likewise, Lys-312 of β-catenin coordinates with Glu-24 of the XTcf3-CBD. The relative strength of these charged interactions is represented with first order equipotential contours included in Figure 3B. The relative contour gradients demonstrate that these two regions of the surface act as the predominant foci of the XTcf3-CBD/β-catenin interaction in the extended region. We call these two lysine residues "charged buttons" since they are strong and specific anchors in the β-catenin groove that fasten XTcf3 to β-catenin.

At one end of the extended region of XTcf3-CBD, Asp-16 and Glu-17 contact Lys-435 (the first button) and Lys-508, respectively (Figure 3C). C-terminal to Asp-16, the XTcf3-CBD peptide chain is aligned in the groove by His-470 and Asn-426 of β-catenin. On one side of the XTcf3-CBD peptide chain, the phenyl ring of conserved Phe-21 is sandwiched between the side chain of Ile-19 and the hydrophobic portion of β-catenin Arg-386. On the other side, Leu-18 sits in a hydrophobic dimple and Arg-20 forms a salt bridge with β-catenin Asp-390. Near the second charged button, the carbonyl and amine groups of Asp-23 coordinate with the polar headgroup of β-catenin Asn-387, stabilizing the binding of Glu-24 to β-catenin Lys-312 (the second button). Residues 25 to 29 of XTcf3 contain three negatively charged residues that interact with the highly positively charged β-catenin groove around armadillo repeat 5 (data not shown).

Interactions between β-Catenin and the Helix of XTcf3-CBD

The helical region of XTcf3-CBD consists of residues Asp-40 to Glu-51. The topography of the complementary β-catenin molecular surface is rather hydrophobic in nature with a shallow hydrophobic pocket (Figure 4A). The helix of XTcf3-CBD lies approximately antiparallel to the third helices of armadillo repeats 3 and 4 in β-catenin, which make up this surface (Figures 1A and 4A). The buried interfacial area is approximately 1200 Å.

The XTcf3-CBD helix consists of the Tcf/LEF-1 family consensus sequence N′-DLA(Ac)(h)KSSLV-C′, where "Ac" denotes an acidic residue and "h" denotes a hydrophobic residue (Figure 1B). The side chains of Asp-40 and Lys-45 of the XTcf3-CBD coordinate with the side chains of Lys-335 and Asn-261 of β-catenin, respectively (Figure 4B). These two interactions may act as tethers to stabilize the relative positioning of the helix. Four hydrophobic residues in the XTcf3-CBD helix, Leu-41, Val-44, Leu-48, and Val-49, form a surface complementary to the β-catenin groove (Figure 4A). Omer et al. previously demonstrated that mutating Leu-48 of Tcf4 to Ala reduces Tcf4's binding affinity for β-catenin (Omer et al., 1999). In our structure, Leu-48 of XTcf3 sits in a

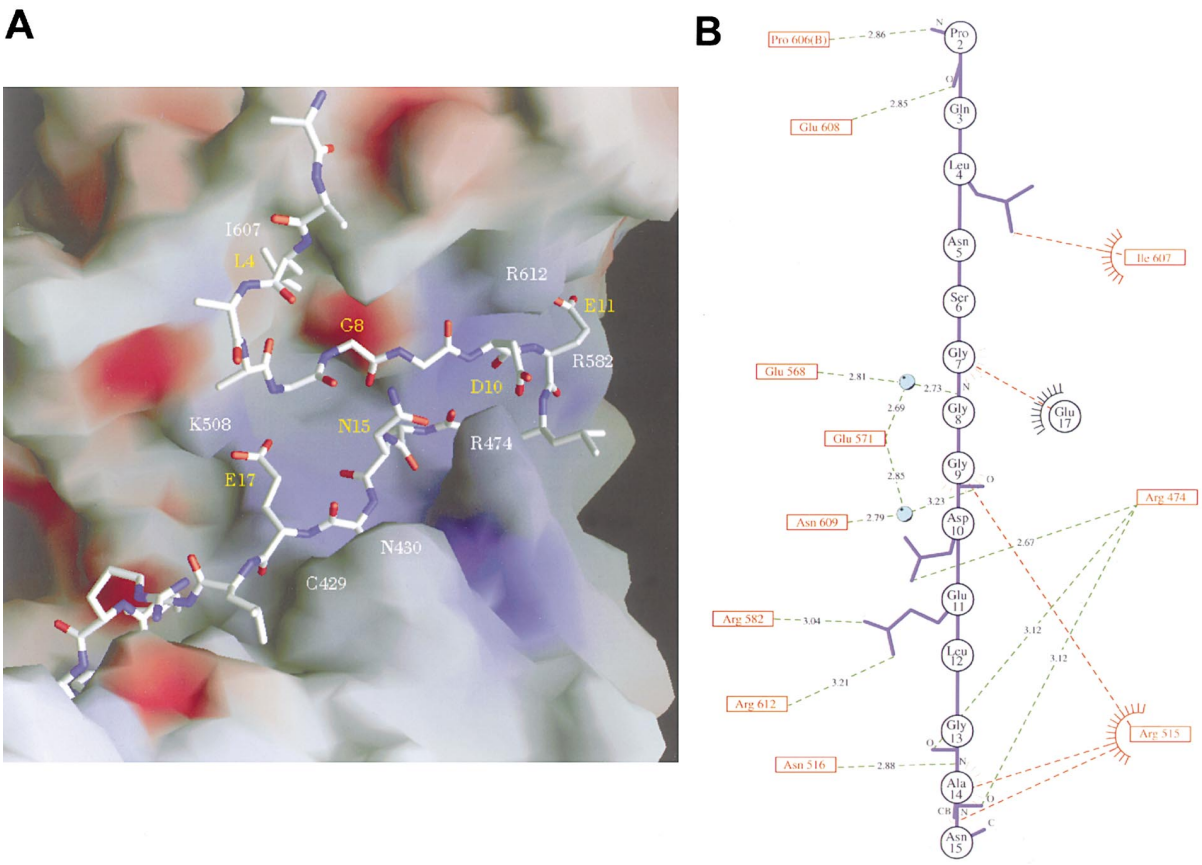

Figure 2. The Interactions between β-Catenin and the β Hairpin Module of XTcf3-CBD

(A) Molecular model of the XTcf3 hairpin module atop the β-catenin molecular surface. The surface is colored according to the relative electrostatic potential, with red denoting negative charge while blue shows positive charge. All electrostatic surfaces in this paper are shown at the same relative level. β-catenin residues are labeled in white and Tcf3 residues are labeled in yellow.

(B) Tcf3 hairpin region bonding diagram. The main chain of XTcf3 is shown in purple and Tcf3 residues are denoted by black circles with black text. β-catenin residues are denoted by red boxes and red text. Hydrophobic interactions are denoted in red, with a "starburst," and hydrogen bonds and charged interactions are denoted in green. Potentially critical solvent molecules are shown in turquoise.

shallow hydrophobic pocket formed by residues Phe-253 and Phe-293 of β-catenin.

Mutational Analysis of the β-Catenin/XTcf3 Interaction

Having determined the structure of the β-catenin/XTcf3 complex, we were able to predict which amino acids in β-catenin might be necessary for Tcf3 binding. In order to test these predictions, we introduced specific amino acid changes into *Xenopus* β-catenin and examined the interaction of these mutants with full-length XTcf3. We specifically targeted residues that interact with the extended region and the C-terminal helical domain of XTcf3. We did not analyze residues in β-catenin that interact with the hairpin region since previous studies have demonstrated that this domain is dispensable for β-catenin binding (Omer et al., 1999).

Within the extended region, interactions between aspartate residues in XTcf3 and lysine residues in β-catenin appear to be of major importance. Asp-16, which was shown to be critically required for the binding of Tcf4 to β-catenin, forms a salt bridge with Lys-435 of β-catenin in our structure (Figure 3B). To test the role of this first charged button in β-catenin/Tcf interactions, we made a lysine to glutamate point mutation in β-catenin at residue 435 (K435E). We produced ^{35}S-labeled XTcf3 and β-catenin-K435E in rabbit reticulocyte lysates, mixed them, and immunoprecipitated the β-catenin with an attached epitope tag. Compared to wild-type β-catenin, the K435E mutant was dramatically reduced in its ability to coimmunoprecipitate XTcf3 in this assay (Figure 5A). In our structure, another tight salt bridge forms between Glu-24 of XTcf3 and Lys-312 of β-catenin (Figure 3B). We substituted a glutamate for this lysine to create a K312E mutant, which was also severely reduced in its ability to interact with XTcf3 (Figure 5A). However, substituting a glutamate for Lys-270, which appears to weakly coordinate with Glu-26 in XTcf3 (not shown), had no appreciable effect on XTcf3 binding (Figure 5A). Our results indicate that lysines 312 and 435 are required to fasten β-catenin to the extended domain of XTcf3.

Unlike the extended region of XTcf3, which appears to rely primarily on charge–charge interactions for its binding to β-catenin, the α helix in XTcf3-CBD binds to a hydrophobic region on the β-catenin surface. In particular, Leu-48 binds in a hydrophobic pocket partly com-

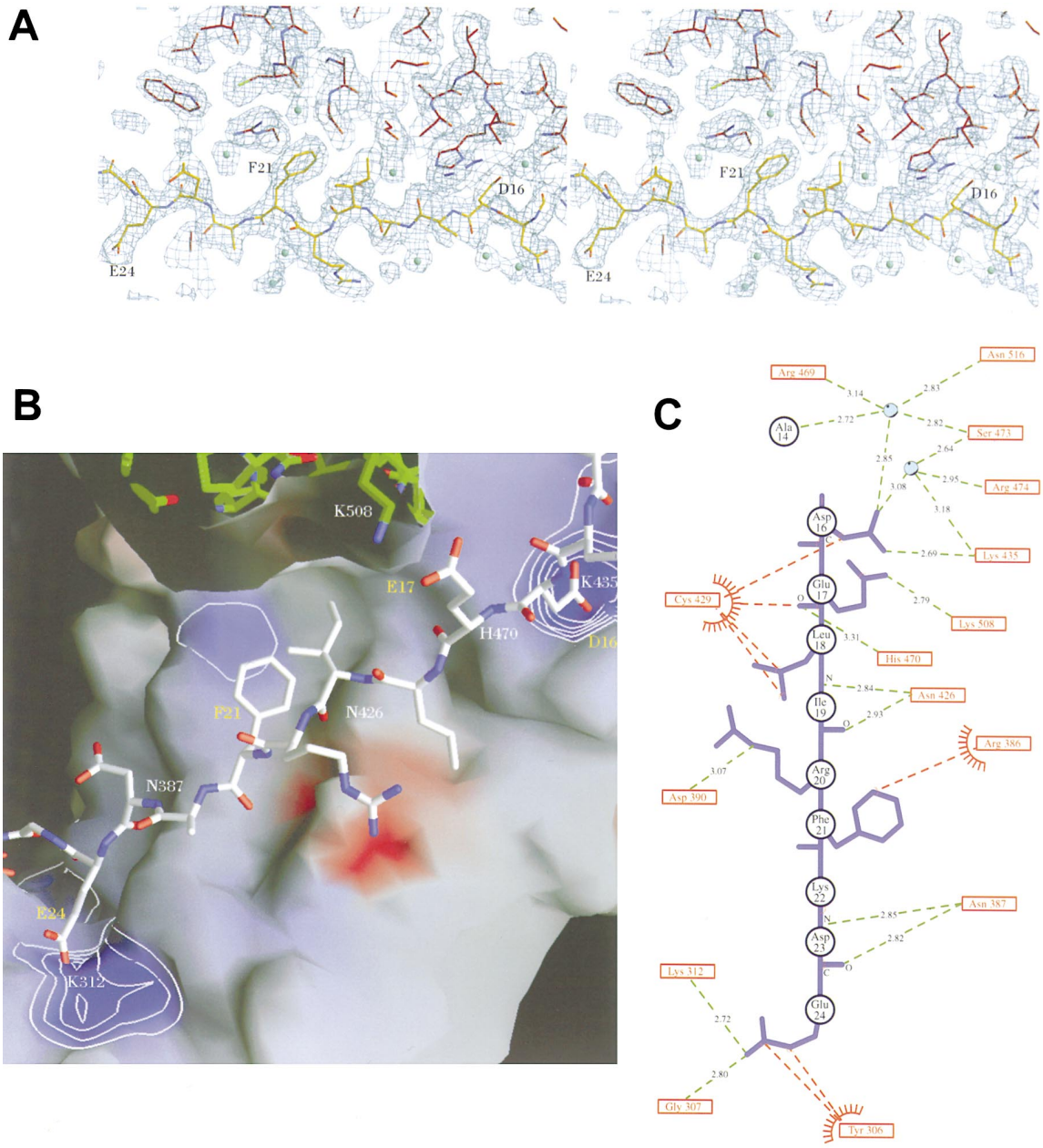

Figure 3. The Interactions between β-Catenin and the β Strand in the Extended Region of XTcf3-CBD

(A) Stereo $2F_o-F_c$ simulated annealed omit map of XTcf3-CBD. XTcf3 residues are denoted in yellow and β-catenin residues are denoted in red. Solvent molecules are shown in turquoise. The map is shown at a level of 1σ.

(B) Structure of the XTcf3 extended region on the top of the β-catenin molecular surface. Two semi-buried charged buttons, Lys-435 and Lys-312, are critical for the β-catenin/Tcf interactions. The β-catenin surface was cut off in the upper part of the figure to be able to view the extended region of XTcf3-CBD. XTcf3 residues are shown in white and exposed β-catenin residues due to the cut surface are shown in green. XTcf3 residues are labeled in yellow and β-catenin residues are labeled in white. The equipotential contours at the relative levels of 10, 20, 30, 40, and 50 were calculated with GRASP and are shown in white.

(C) XTcf3 extended region bonding diagram. The same conventions are used as in Figure 2B.

posed of Phe-253 and Phe-293. To test the importance of this hydrophobic pocket in β-catenin/Tcf interactions, we introduced a phenylalanine to aspartate mutation in β-catenin at residue 253 (F253D) that partly reduced its ability to interact with XTcf3 (Figure 5A). In order to further disrupt the hydrophobic pocket, we also changed Phe-293 to an aspartate, creating a double mutant (F253D/F293D) within the pocket. These combined mutations, which may alter both the shape and the hydrophobicity of the pocket, strongly inhibited XTcf3 binding to β-catenin (Figure 5B).

We also attempted to disrupt binding by mutating Ala-295 and Ile-296 of β-catenin to tryptophans, which are predicted to form a "dam" jutting up from the floor of

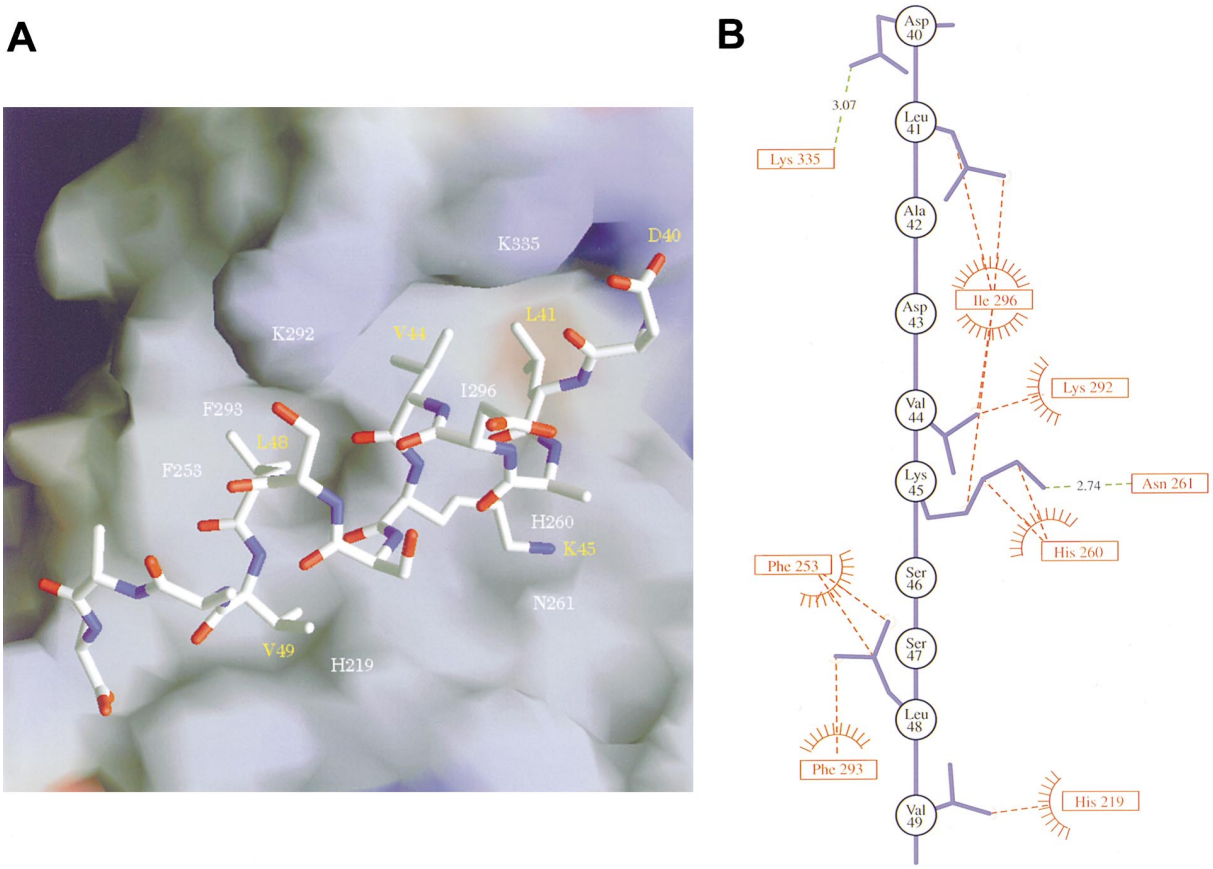

Figure 4. The Interactions between β-Catenin and the XTcf3-CBD Helix

(A) Molecular model of the XTcf3 helical region. XTcf3 residues are labeled in yellow and β-catenin residues are labeled in white.
(B) XTcf3 helix module bonding diagram. The same conventions are used as in Figure 2B.

the groove that blocks the entrance to the hydrophobic region of the groove. In line with our prediction, the A295W/I296W mutation abrogated XTcf3 binding activity (Figure 5B). These mutational results demonstrate that the binding of β-catenin to XTcf3 depends on both the helical region and the extended region of XTcf3-CBD.

Shared Interactions among XTcf3, C-Cadherin, APC, and Axin

Having defined the critical amino acids of β-catenin required for interacting with XTcf3, we asked whether the same residues might be involved in binding the other partners of β-catenin. β-catenin mutants with reduced XTcf3 binding were first tested for their ability to interact with full-length *Xenopus* C-cadherin. Interestingly, the same charged buttons used to bind XTcf3 to β-catenin were also required for the binding of C-cadherin to β-catenin (Figure 6A, K312E and K435E). In contrast, the corresponding mutations that interfered with the binding of the XTcf3 helical region with the β-catenin hydrophobic pocket had no effect on the binding of C-cadherin to β-catenin (Figure 6A, F253D, F253D/F293D, and A295W/I296W). Therefore, the binding sites of XTcf3 on β-catenin only partially overlap with those of C-cadherin.

We next examined the interaction of APC with the mutant β-catenins. The central region of *Xenopus* APC (XAPC) contains two conserved 15 amino acid repeats and seven conserved 20 amino acid repeats that are important for β-catenin binding. Since APC is a very large protein, it is not effectively produced in vitro. We therefore used a fragment of XAPC, XAPC4, that contains one of the 15 amino acid repeats and five of the 20 amino acid repeats (Vleminckx et al., 1997). As with C-cadherin, point mutations in the charged buttons of β-catenin reduced the binding of XAPC4 to β-catenin (Figure 6B, K312E and K435E). Intriguingly, mutations that prevented the binding of the XTcf3 helix also dramatically reduced the binding of XAPC4 to β-catenin (Figure 6B, F253D/F293D and A295W/I296W). These results demonstrate that similar amino acids in β-catenin are used to bind Tcf3 and APC.

Finally, we examined the binding of *Xenopus* Axin (XAxin) to the β-catenin mutants. Unlike C-cadherin and APC, the binding of XAxin to β-catenin does not depend on the Lys-312 or Lys-435 buttons (Figure 6C). However, the binding of XAxin to β-catenin was disrupted by the mutations F253D/F293D and A295W/I296W that prevent binding of the XTcf3-CBD helix (Figure 6C). Remarkably, introducing a single amino acid substitution into the hydrophobic pocket (F253D), which was not sufficient to prevent C-cadherin or XAPC4 binding, was as effective as the double mutations at inhibiting the binding of

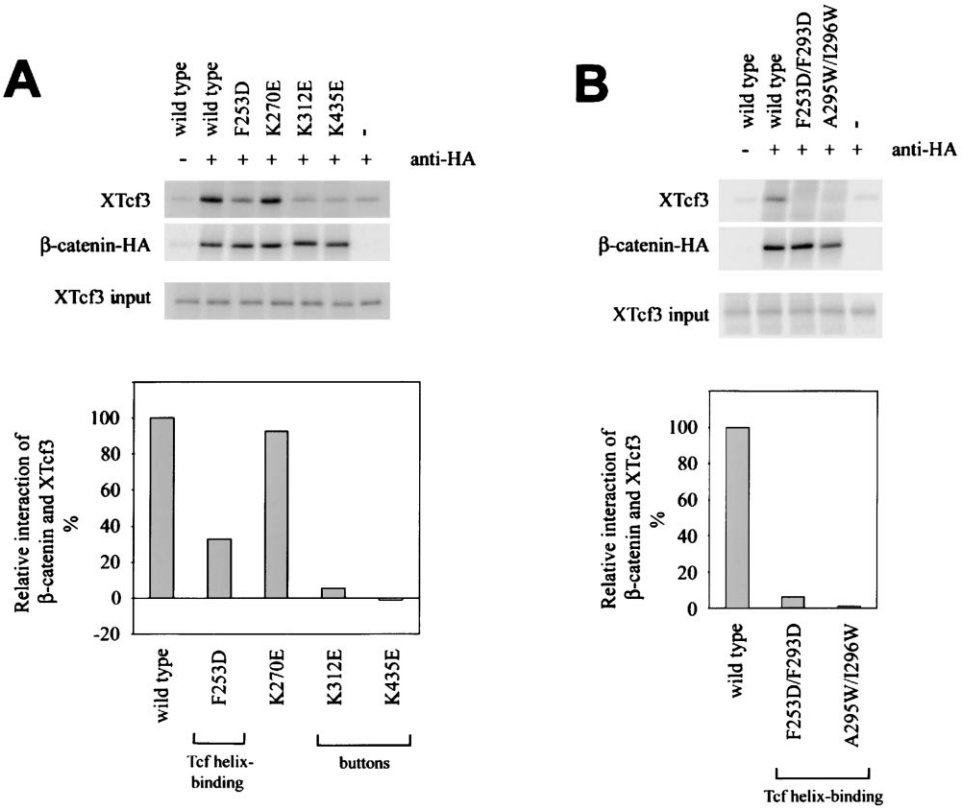

Figure 5. Mutational Analysis of β-Catenin/XTcf3 Interaction

In vitro translated, ^{35}S-labeled, full-length XTcf3 and HA-tagged β-catenin were mixed and immunoprecipitated with an anti-HA antibody. The input represents 4% of the mixed proteins, removed prior to immunoprecipitation. Relative intensities of the XTcf3 bands are shown below the autoradiographs, with 100% representing the amount of XTcf3 bound to wild-type β-catenin.

(A) Analysis of single point mutations.

(B) Analysis of double point mutations.

XAxin to β-catenin (Figure 6C). These results demonstrate that the binding region of Axin on β-catenin overlaps that of the XTcf3-CBD helix, but not that of the extended region.

Discussion

As seen in the β-catenin/Tcf complex crystal structure, β-catenin provides a rigid platform that presents main chain and side chain groups for Tcf recognition. The armadillo repeat region forms an ideal structural platform that restrains the positions of Cβ atoms as well as all main chain atoms. In this sense, β-catenin is analogous to double-stranded DNA. It forms a right-handed superhelix with a groove that spirals along the helix. The β-catenin binding domain of XTcf3 (XTcf3-CBD) extends along much of this groove, binding to β-catenin with three different modules. Recognition of a peptide spread out in a rigid groove allows the peptide to bind with high specificity by exposing all its functional groups for recognition. In addition, binding in the groove allows a higher binding affinity due to a larger protein–protein interface—the K_d between β-catenin and hTcf4-CBD is in a low nM range (Omer et al., 1999). Since all of the critical residues in our β-catenin/Tcf3 interface are conserved in the Tcf/LEF-1 family, we expect that the binding mode observed in our structure serves as a framework for all β-catenin/Tcf and β-catenin/LEF-1 interactions. Furthermore, our β-catenin/Tcf-CBD structure, together with our mutagenesis data, suggest that binding within the groove of the armadillo repeat region of β-catenin may be a common theme for some other CBDs, such as those of cadherins and APC (see below). It is noteworthy that another armadillo repeat protein, Karyopherin, also uses its groove to recognize NLS (nuclear localization signal) peptides in extended conformations (Conti et al., 1998).

Structural Determinants of β-Catenin-Tcf Interactions

The XTcf3-CBD can be roughly divided into three binding modules: an N-terminal β hairpin (residues 7–15), an extended region that contains two charged "buttons" (residues 16–29), and an α helix (residues 40–52). Our crystal structure and the previous Tcf4 mutagenesis data allowed us to locate three hot spots at the β-catenin/Tcf3 interface that are critical for the binding of XTcf3 to β-catenin. Two of them are charged buttons in which the lysine residues at postions 312 and 435 bind acidic residues in the extended region of the XTcf3-CBD. The other hot spot is a hydrophobic pocket that binds Leu-48 of XTcf3. By inserting two negatively charged aspartate

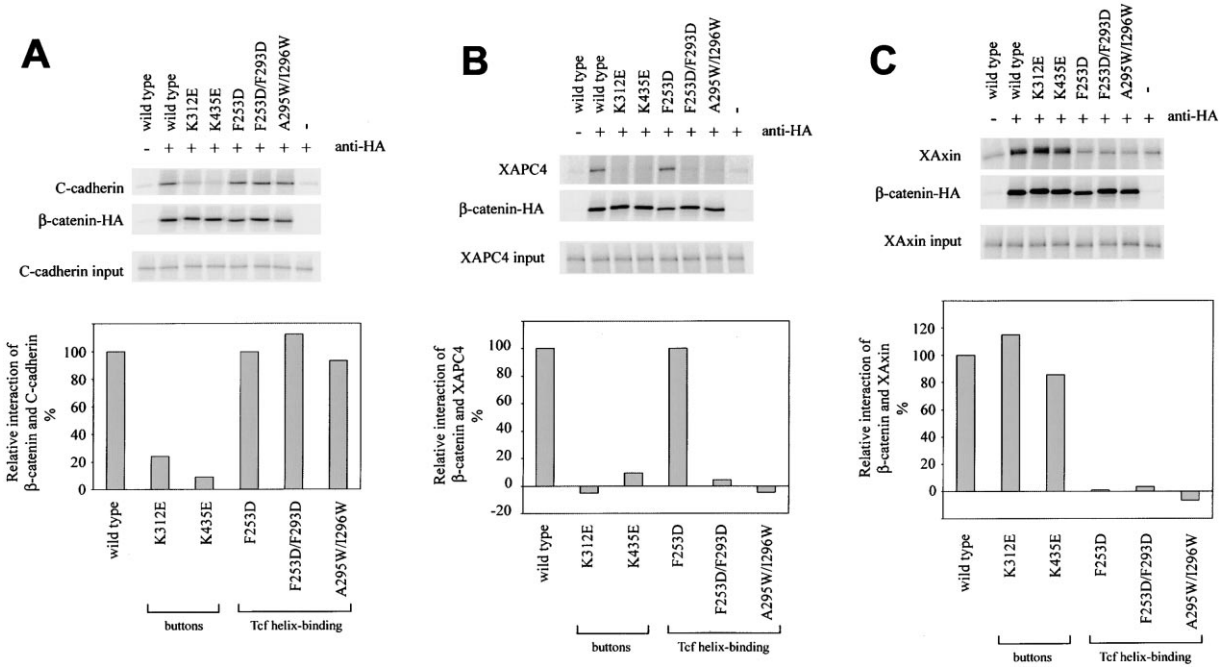

Figure 6. Interaction of β-Catenin Mutants with C-Cadherin, XAPC4, and Xaxin

In vitro translated, ^{35}S-labeled HA-tagged β-catenin was mixed with in vitro translated, ^{35}S-labeled *Xenopus* C-cadherin, XAPC4, or XAxin. Samples were immunoprecipitated with an anti-HA antibody. The input represents 4% of the mixed proteins, removed prior to immunoprecipitation. Relative intensities of the C-cadherin, XAPC4, or XAxin bands are shown below the relevant autoradiographs, with 100% representing the amount of each protein bound to wild-type β-catenin.

(A) Analysis of C-cadherin binding.

(B) Analysis of XAPC4 binding.

(C) Analysis of XAxin binding.

residues in this hydrophobic pocket, we were able to prevent XTcf3 from binding β-catenin. In addition, to mimic the effects of a small compound bound in the groove of β-catenin, in which the α helix docks, we designed a double mutation to build a "dam" in the β-catenin groove. This A295W/I296W mutation also prevented XTcf3 binding to β-catenin.

Our results are completely consistent with previously reported Tcf4 mutagenesis data (Omer et al., 1999). Omer et al. produced a series of peptides of the human Tcf4 CBD containing deletions and mutations at conserved residues, and measured the ability of these mutant peptides to compete with the wild-type Tcf4 peptide for β-catenin binding. Because of the high similarity between human Tcf4 and *Xenopus* Tcf3 (Figure 1B), we can readily map their results onto our structure. This comparison demonstrates that the extended region of Tcf is the minimal unit for binding to β-catenin (see also von Kries et al., 2000), whereas the β hairpin region is largely dispensable. The α helix makes important contributions to the binding affinity of Tcf4 to β-catenin, since a mutation in this region dramatically reduces the binding affinity of the Tcf4 CBD for β-catenin. Based on these results, we suggest that the docking of the extended region to the positively charged groove of β-catenin may be the first step in the β-catenin/Tcf recognition, and that the subsequent binding of the α helix to β-catenin through hydrophobic interactions provides a critical component of the high affinity binding.

In general, the formation of secondary structure may restrain the conformation of a peptide chain and thus allow the protein to present its surface features in a more specific manner. It is interesting to note that the β-catenin binding domain of XTcf3 contains a β hairpin module and an α helix at the N- and C-terminal ends, respectively, flanking the essential central extended region. One of the features of the β-catenin/Tcf interaction is that, while the central extended region provides the minimal recognition domain, the two flanking structural modules appear to help restrain the central extended region to binding in its docking site. In the β-catenin/XTcf3 structure, the residues C-terminal to Glu-29 of XTcf3 are quite flexible and can potentially be stretched. This helps to explain a paradox in the mutagenesis data. While mutation of the second charged button of β-catenin (K312D) abolished the binding to XTcf3, the corresponding mutation in Tcf4 (E24A) did not have dramatic effects on β-catenin/Tcf4 binding (Omer et al., 1999). It is interesting to note that there are several negatively charged residues (Glu-26, Glu-28, and Glu-29) C-terminal to Glu-24. It is possible that residues in this region can adopt alternative conformations so that another negatively charged residue can match with the Lys-312 button when Glu-24 is mutated.

Interactions of β-Catenin with APC, Cadherin, and Axin

β-catenin plays multiple roles in cell regulation by forming complexes with more than two dozen protein partners (Zhurinsky et al., 2000). We were interested to know

whether any of the β-catenin residues required for interacting with XTcf3 are also used to bind other well-defined CBDs of different partners, even though there was no apparent reported sequence homology. Of the proteins we tested, APC behaved most like XTcf3. Mutations in the region that binds the XTcf3 helix, as well as in the button region, significantly impair APC binding. In contrast, C-cadherin binding to β-catenin requires the buttons but is not affected by mutations that inhibit binding of the XTcf3 helix. This is in agreement with deletion studies demonstrating that armadillo repeats 1–3, which include residues that bind the XTcf3 helix, are not required for E-cadherin binding (Pai et al., 1996). Finally, Axin does not bind to the β-catenin buttons defined here, but does require contact with the XTcf3 helix binding region. Intriguingly, a single amino acid change in the hydrophobic pocket that interacts with the helix (F253D) is not sufficient to abrogate cadherin or APC binding, but does prevent the binding of Axin to β-catenin. This result indicates that Axin/β-catenin binding is more dependent on an interaction in the hydrophobic region than cadherin/β-catenin or APC/β-catenin binding, which may be due to the absence of interactions between Axin and the β-catenin buttons. Our observations that these proteins share overlapping binding sites are consistent with earlier reports that binding of Tcf, APC, and cadherin is mutually exclusive (Hulsken et al., 1994; Rubinfeld et al., 1995; Orsulic and Peifer, 1996). Since Axin and APC can simultaneously bind to β-catenin (Hart et al., 1998; Salic et al., 2000), it is plausible that APC can utilize the charged buttons for binding while at the same time Axin might bind to the helical binding region of β-catenin.

While this manuscript was in preparation, von Kries et al. reported the effects of individually mutating 18 charged and hydrophobic amino acids within the groove of the β-catenin superhelix on the binding of LEF-1, APC, and Conductin (a relative of Axin) (von Kries et al., 2000). Three of their mutagenized residues overlapped with those we targeted, and while our results generally agree with theirs at these three sites, our overall conclusion is different. Based on their mutagenesis data, they conclude that different β-catenin binding partners bind unique localized clusters of amino acids on β-catenin, which they termed hot spots. For example, they propose that LEF-1 binds a unique cluster near armadillo repeat 8 of β-catenin, which contains the Lys-435 charged button. In contrast, our structural data demonstrate that XTcf3 binds at multiple regions along β-catenin, and our mutagenesis data show that multiple residues are shared among different β-catenin binding partners. The major reason for the differences between the conclusions of these mutagenesis studies is that our mutations were based on an analysis of the structure. For example, using equipotential contours, we defined the button at Lys-312 and showed that it is important for the binding of three of the four proteins tested, whereas this residue was not examined in the other work.

Von Kries et al. produced two β-catenin mutations that we did not make, R469A and H470A, which disrupted LEF-1 binding (von Kries et al., 2000). Arg-469 is important for stabilizing the Asp-16 side chain of XTcf3, whereas His-470 guides the main chain of Glu-17 along the groove of β-catenin (Figure 3C). The one discrepancy between our work and that of von Kries et al. is that we saw a strong effect of mutations at Lys-435 on APC binding, whereas they saw only a minimal effect. One potential difference is that they used small fragments of APC that contained either the 15 or 20 amino acid repeats, whereas we used a much larger fragment that contained both types of repeats.

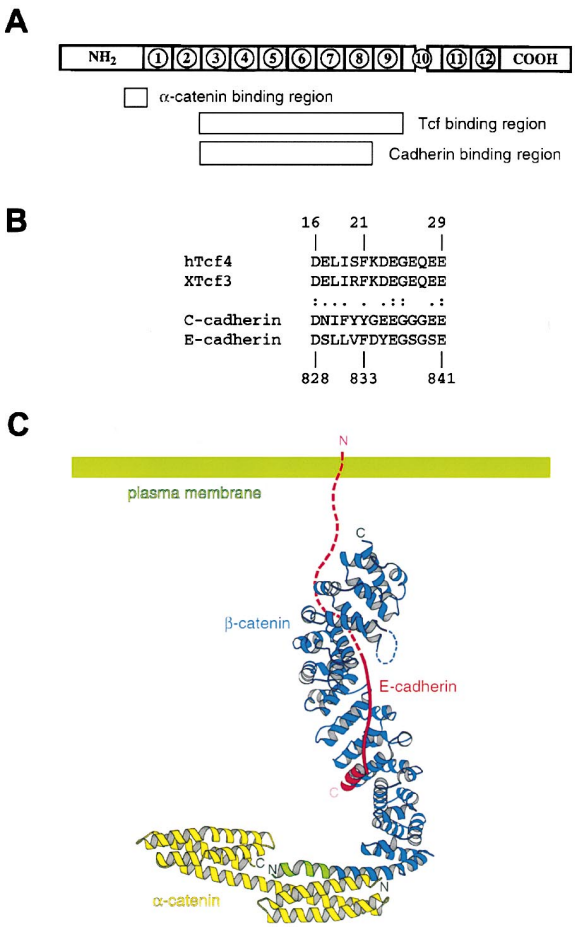

Figure 7. A Proposed Model of the E-Cadherin/β-Catenin/α-Catenin Complex

(A) The β-catenin binding sites of α-catenin, Tcf, and cadherin, based on previous truncation experiments. Note that the β-catenin binding sites of Tcf and cadherin are overlapping.

(B) Sequence alignment of the extended region of Tcf-CBDs with the N-terminal half of cadherin-CBDs.

(C) An illustration of a proposed model for the E-cadherin/β-catenin/α-catenin complex. Our β-catenin structure is in indigo. The β-catenin binding region of α-catenin (in yellow) is aligned to β-catenin by superimposing our β-catenin structure onto residues 134–141 of the β-catenin helix in an α/β-catenin chimera structure (Pokutta and Weis, 2000). A portion of the β-catenin helix in the α/β-catenin chimera structure, which is not included in our β-catenin/XTcf3 structure, is shown in green. The orientation of the N-terminal half of E-cadherin-CBD (red) is based on the sequence alignment shown in Figure 7B. The C-terminal half of E-cadherin-CBD may contain an α helix as suggested by secondary structure predictions, and is docked on a positively charged area in the β-catenin groove. For simplicity, the extracellular region of E-cadherin is not shown.

Similarities in the Tcf and Cadherin CBDs

Previous truncation studies suggested that Tcf and cadherin bind to corresponding regions of β-catenin (Figure 7A) (Hulsken et al., 1994; Behrens et al., 1996;

Molenaar et al., 1996; Orsulic and Peifer, 1996; Pai et al., 1996). Although no apparent homology was found between Tcf-CBD and the cadherin-CBD, the similar requirement of XTcf3 and C-cadherin for binding to the charged buttons, Lys-312 and Lys-435, suggests that they may share a conserved β-catenin binding motif. It has been shown that an ~30 amino acid region in the E-cadherin cytoplasmic domain is necessary and sufficient for β-catenin binding (Stappert and Kemler, 1994; Pai et al., 1996). The N-terminal half of the cadherin-CBD is remarkably similar in sequence to the critical extended region of Tcf4-CBD that binds the charged buttons. In particular the two button binding residues in XTcf3-CBD (Asp-16 and Glu-24), as well as a critical residue identified in LEF-1 (corresponding to Phe-21 in XTcf3; Von Kries et al., 2000), are also conserved in the cadherin-CBD (Figure 7B). Thus, we propose that the N-terminal half of the cadherin-CBD binds to β-catenin in a conformation similar to that of the extended region of the XTcf3-CBD (Figure 7C).

A Structural Model for the Cadherin/β-Catenin/α-Catenin Complex in Cell Adhesion

α-catenin is an essential link between adhesion junctions and the cytoskeleton. While the N-terminal region of α-catenin is responsible for interacting with β-catenin, its C-terminal region binds to actin, directly or via α-actinin. α-catenin binds to the junction of the N-terminal domain and the armadillo repeat region of β-catenin. Biochemical studies and a crystal structure of a chimeric protein of α-catenin (residue 57–164) and β-catenin (residues 118–151) have resulted in a model for the interaction of the β-catenin junction segment with α-catenin (Aberle et al., 1996; Pokutta and Weis, 2000). In the crystal structure of the α-/β-catenin chimera, residues 121–141 of β-catenin form an α helix, and this helix interacts with three α helices in α-catenin by forming a four-helix bundle. Since the residues N-terminal of residue 150 were not visible in the earlier reported crystal structures of the armadillo repeat region of murine β-catenin, it was not possible to predict the relative orientation between α- and β-catenin. In our crystal structure, we were able to visualize residues 134–149, and show that amino acids 134–161 form a long kinked helix (Figure 7C).

Although we could not view the structure beyond residue 134, which is the first amino acid in our construct, the structure of this region in the chimeric protein indicates that this helix continues further toward the N terminus of β-catenin. Since α-catenin binds this helix in a four-helix bundle, this orients α-catenin approximately perpendicular to the β-catenin superhelix (Figure 7C). Consolidating the E-cadherin/β-catenin complex and β-catenin/α-catenin complex models, E-cadherin and α-catenin sit on roughly opposite surfaces of β-catenin. In addition, because we suggest that the E-cadherin peptide chain runs antiparallel to the groove of the armadillo repeat superhelix, the N terminus of β-catenin, and thus α-catenin, are pointing away from the plasma membrane (Figure 7C).

Prospects for Drug Design

Since the inappropriate activation of the Wnt pathway is implicated in numerous cancers, it will be of great interest to develop reagents that can specifically inhibit this pathway. As these cancers result from abnormally high levels of β-catenin, it is necessary to develop reagents that act downstream of β-catenin. Disrupting the interaction between Tcf and β-catenin is one promising avenue, as long as this does not prevent the formation of the cadherin/β-catenin complex, which would result in aberrant cell adhesion.

Our structural and mutagenesis studies suggest that the region of β-catenin that binds the XTcf3 helix might be a promising place for the design of small molecule inhibitors. There is a hydrophobic pocket lined by Phe-253 and Phe-293 that is required for XTcf3 to bind β-catenin. Mutations in this pocket, or in the shallow groove nearby, had no effect on C-cadherin binding, indicating that a drug binding in this region might not be deleterious for cell adhesion. As with all chemotherapy agents, the key issue will be to develop molecules and conditions that will adversely impact the cancer cells without harming normal cells.

Experimental Procedures

Data Collection and Structure Determination

The β-catenin/XTcf3-CBD complex was purified and crystallized as described (F. M. et al., unpublished data). A 2.1 Å resolution data set was collected from the Beamline 5.0.2 at ALS (Advanced Light Source), and processed with Denzo and Scalepack (Otwinowski and Minor, 1997). The space group is $P2_12_12_1$ with the unit cell a = 52.14 Å, b = 153.25 Å, and c = 188.12 Å. Molecular replacement was carried out via AmoRe (Navaza, 1994). The search model was the armadillo repeat region of the murine β-catenin (entry 3BCT from PDB). The rotation and translation search gave two independent solutions within the asymmetric unit. The final correlation function and R factor after molecular replacement are 54.1% and 40.1%.

Refinement and model building were carried out with CNS (Brunger et al., 1998) and Xtalview (McRee, 1999). 8.4% of the reflections were put aside as the test set and a 2σ cutoff was applied throughout refinement. After rigid body refinement, the model was built with rounds of manual rebuilding, positional refinement, simulated annealing, and individual B factor refinement. The stereochemical quality of the model was monitored via Procheck (Laskowski et al., 1993). The final model R factors, after applying anisotropic B factor and isotropic bulk solvent corrections, are R_{work} = 22.9% and R_{free} = 25.5%. The protein complex model is 94% complete for one of the solutions and 79% complete for the other. 95.6% of the 1039 modeled residues lie within the most favored regions of the Ramachandran plot, and none in the disallowed regions.

The relative equipotential contours of the β-catenin molecular surface, shown in Figure 3B, were calculated with the finite difference poisson-boltzmann solver of GRASP (Nicholls et al., 1991). The inner dielectric parameter was set to 2.0 and the outer, or solvent, dielectric parameter was set to 80 with the interface defined by a solvent probe size of 1.4 Å. The calculation was done in the absence of XTcf3.

In Vitro Translation and Coimmunoprecipitation Assay

Xenopus β-catenin-HA was described previously (Farr et al., 2000). Site-directed mutagenesis of β-catenin was carried out using the QuikChange procedure (Stratagene), except that Platinum Pfx (Gibco BRL) was used in place of Pfu. XTcf3 (Molenaar et al., 1996), *Xenopus* C-cadherin (Levine et al., 1994), XAPC4 (Vleminckx et al., 1997), and Xaxin-myc (Hedgepeth et al., 1999) were as described. *Xenopus* β-catenin-HA, XTcf3, C-cadherin, XAPC4, and XAxin-myc constructs were in vitro transcribed and translated using the TNT SP6 coupled rabbit reticulocyte lysate system (Promega). Rabbit reticulocyte lysate containing ^{35}S methionine-labeled wild-type or mutant β-catenin proteins were mixed with equal amounts of lysates containing ^{35}S methionine-labeled XTcf3, XAPC4, C-cadherin, or XAxin-myc, and nutated at 4°C for 1 hr. Anti-HA antibody (BABCO

or Santa Cruz Biotechnology) was added to each sample, except for the negative controls, and rotated at 4°C for 1 hr. Protein G sepharose beads (Pharmacia) were subsequently added to each sample, followed by another 1 hr incubation with nutation. Beads were washed three times in the following buffers before sample preparation: for XTcf3, 0.1% Triton X-100, 0.02% SDS, 150 mM NaCl, 50 mM Tris-HCl, pH 7.4, 5 mM EDTA. For C-cadherin and XAPC4, 0.5% NP-40, 150 mM NaCl, 20 mM Tris-HCl, pH 8. For XAxin-myc, 1% Triton X-100, 1% DOC, 0.1% SDS, 150 mM NaCl, 10 mM Tris-HCl, pH 7.2. Samples were eluted with 20 μl of SDS-PAGE sample buffer and run on a 7.5% acrylamide gel. Bands were visualized using the Storm Imaging System (Molecular Dynamics).

Acknowledgments

We are grateful to B. Stoddard and E. Galburt for synchrotron data collection; to W. Hol for helpful discussions; and to B. Stoddard, J. Clark, and D. Raible for critical comments on the manuscript. We also thank X. He, C. Liu, P. Klein, P. McCrea, and B. Gumbiner for constructs, and S. Turley and C. A. Ward for technical assistance. This work was supported by NIH grant HD27262 to D. K. and a New Investigator Grant from the Leukemia Research Foundation to W. X.; T. G. and C. W. were supported by NIH training grants GM07270 and HD07183, respectively.

Received October 10, 2000; revised October 30, 2000.

References

Aberle, H., Schwartz, H., Hoschuetzky, H., and Kemler, R. (1996). Single amino acid substitutions in proteins of the armadillo gene family abolish their binding to α-catenin. J. Biol. Chem. *271*, 1520–1526.

Barker, N., Morin, P.J., and Clevers, H. (2000). The Yin-Yang of TCF/β-catenin signaling. Adv. Cancer Res. *77*, 1–24.

Behrens, J., von Kries, J.P., Kuhl, M., Bruhn, L., Wedlich, D., Grosschedl, R., and Birchmeier, W. (1996). Functional interaction of β-catenin with the transcription factor LEF-1. Nature *382*, 638–642.

Bienz, M., and Clevers, H. (2000). Linking colorectal cancer to wnt signaling. Cell *103*, 311–320.

Brunger, A.T., Adams, P.D., Clore, G.M., DeLano, W.L., Gros, P., Grosse-Kunstleve, R.W., Jiang, J.S., Kuszewski, J., Nilges, M., Pannu, N.S., et al. (1998). Crystallography & NMR system: A new software suite for macromolecular structure determination. Acta Crystallogr. D *54*, 905–921.

Conti, E., Uy, M., Leighton, L., Blobel, G., and Kuriyan, J. (1998). Crystallographic analysis of the recognition of a nuclear localization signal by the nuclear import factor karyopherin . Cell *94*, 193–204.

Farr, G.H., 3rd, Ferkey, D.M., Yost, C., Pierce, S.B., Weaver, C., and Kimelman, D. (2000). Interaction among GSK-3, GBP, Axin, and APC in *Xenopus* axis specification. J. Cell Biol. *148*, 691–702.

Hart, M.J., de los Santos, R., Albert, I.N., Rubinfeld, B., and Polakis, P. (1998). Downregulation of β-catenin by human Axin and its association with the APC tumor suppressor, β-catenin and GSK3. Curr. Biol. *8*, 573–581.

Hecht, A., Litterst, C.M., Huber, O., and Kemler, R. (1999). Functional characterization of multiple transactivating elements in β-catenin, some of which interact with the TATA-binding protein in vitro. J. Biol. Chem. *274*, 18017–18025.

Hecht, A., Vleminckx, K., Stemmler, M.P., van Roy, F., and Kemler, R. (2000). The p300/CBP acetyltransferases function as transcriptional coactivators of β-catenin in vertebrates. EMBO J. *19*, 1839–1850.

Hedgepeth, C.M., Deardorff, M.A., and Klein, P.S. (1999). *Xenopus* Axin interacts with glycogen synthase kinase-3 and is expressed in the anterior midbrain. Mech. Dev. *80*, 147–151.

Huber, A.H., Nelson, W.J., and Weis, W.I. (1997). Three-dimensional structure of the armadillo repeat region of β-catenin. Cell *90*, 871–882.

Hulsken, J., Birchmeier, W., and Behrens, J. (1994). E-cadherin and APC compete for the interaction with β-catenin and the cytoskeleton. J. Cell Biol. *127*, 2061–2069.

Ikeda, S., Kishida, S., Yamamoto, H., Murai, H., Koyama, S., and Kikuchi, A. (1998). Axin, a negative regulator of the Wnt signaling pathway, forms a complex with GSK-3 and β-catenin and promotes GSK-3-dependent phosphorylation of β-catenin. EMBO J. *17*, 1371–1384.

Kato, Y., Shi, Y., and He, X. (1999). Neuralization of the *Xenopus* embryo by inhibition of p300/ CREB-binding protein function. J. Neurosci. *19*, 9364–9373.

Kinzler, K.W., and Vogelstein, B. (1996). Lessons from hereditary colorectal cancer. Cell *87*, 159–170.

Korinek, V., Barker, N., Morin, P.J., van Wichen, D., de Weger, R., Kinzler, K.W., Vogelstein, B., and Clevers, H. (1997). Constitutive transcriptional activation by a β-catenin-Tcf complex in APC−/− colon carcinoma. Science *275*, 1784–1787.

Kraulis, P.J. (1991). MOLSCRIPT: a program to produce both detailed and schematic plots of Protein structure. J. Appl. Crystallogr. *24*, 946–950.

Laskowski, R.A., MacArthur, M.W., Moss, D.S., and Thornton, J.M. (1993). PROCHECK: a program to check the stereochemical quality of protein structures. J. Appl. Crystallogr. *26*, 283–291.

Levine, E., Lee, C.H., Kintner, C., and Gumbiner, B.M. (1994). Selective disruption of E-cadherin function in early *Xenopus* embryos by a dominant negative mutant. Development *120*, 901–909.

McRee, D.E. (1999). XtalView/Xfit—A versatile program for manipulating atomic coordinates and electron density. J. Struct. Biol. *125*, 156–165.

Merritt, E.A., and Murphy, M.E.P. (1994). RASTER3D version 2.0. A program for photorealistic molecular graphics. Acta Crystallogr. D *50*, 869–873.

Molenaar, M., van de Wetering, M., Oosterwegel, M., Peterson-Maduro, J., Godsave, S., Korinek, V., Roose, J., Destree, O., and Clevers, H. (1996). XTcf-3 transcription factor mediates β-catenin-induced axis formation in *Xenopus* embryos. Cell *86*, 391–399.

Moon, R.T., and Kimelman, D. (1998). From cortical rotation to organizer gene expression: toward a molecular explanation of axis specification in *Xenopus*. Bioessays *20*, 536–545.

Morin, P.J. (1999). β-catenin signaling and cancer. Bioessays *21*, 1021–1030.

Navaza, J. (1994). AMoRe: an automated package for molecular replacement. Acta Crystallogr. A *50*, 157–163.

Nicholls, A., Sharp, K.A., and Honig, B. (1991). Protein folding and association: insights from the interfacial and thermodynamic properties of hydrocarbons. Proteins *11*, 281–296.

Omer, C.A., Miller, P.J., Diehl, R.E., and Kral, A.M. (1999). Identification of Tcf4 residues involved in high-affinity β-catenin binding. Biochem. Biophys. Res. Commun. *256*, 584–590.

Orsulic, S., and Peifer, M. (1996). An in vivo structure-function study of armadillo, the β-catenin homologue, reveals both separate and overlapping regions of the protein required for cell adhesion and for wingless signaling. J. Cell Biol. *134*, 1283–1300.

Otwinowski, Z., and Minor, W. (1997). Processing of X-ray diffraction data collected in oscillation mode, Volume 276, C.W.J. Carter and R.M. Sweet, eds. (New York: Academic Press).

Pai, L.M., Kirkpatrick, C., Blanton, J., Oda, H., Takeichi, M., and Peifer, M. (1996). *Drosophila* α-catenin and E-cadherin bind to distinct regions of *Drosophila* Armadillo. J. Biol. Chem. *271*, 32411–32420.

Peifer, M., and Polakis, P. (2000). Wnt signaling in oncogenesis and embryogenesis—a look outside the nucleus. Science *287*, 1606–1609.

Pokutta, S., and Weis, W.I. (2000). Structure of the dimerization and α-catenin-binding region of β-catenin. Mol. Cell *5*, 533–543.

Polakis, P. (2000). Wnt signaling and cancer. Genes Dev. *14*, 1837–1851.

Provost, E., and Rimm, D.L. (1999). Controversies at the cytoplasmic face of the cadherin-based adhesion complex. Curr. Opin. Cell Biol. *11*, 567–572.

Roose, J., and Clevers, H. (1999). TCF transcription factors: molecu-

lar switches in carcinogenesis. Biochim. Biophys. Acta *1424*, M23–M37.

Rubinfeld, B., Souza, B., Albert, I., Munemitsu, S., and Polakis, P. (1995). The APC protein and E-cadherin form similar but independent complexes with α-catenin, β-catenin, and plakoglobin. J. Biol. Chem. *270*, 5549–5555.

Salic, A., Lee, E., Mayer, L., and Kirschner, M.W. (2000). Control of β-catenin stability: reconstitution of the cytoplasmic steps of the wnt pathway in *Xenopus* egg extracts. Mol. Cell *5*, 523–532.

Seidensticker, M.J., and Behrens, J. (2000). Biochemical interactions in the wnt pathway. Biochim. Biophys. Acta *1495*, 168–182.

Stappert, J., and Kemler, R. (1994). A short core region of E-cadherin is essential for catenin binding and is highly phosphorylated. Cell Adhes. Commun. *2*, 319–327.

Takemaru, K.I., and Moon, R.T. (2000). The transcriptional coactivator CBP interacts with β-catenin to activate gene expression. J. Cell Biol. *149*, 249–254.

van de Wetering, M., Cavallo, R., Dooijes, D., van Beest, M., van Es, J., Loureiro, J., Ypma, A., Hursh, D., Jones, T., Bejsovec, A., et al. (1997). Armadillo coactivates transcription driven by the product of the *Drosophila* segment polarity gene dTCF. Cell *88*, 789–799.

Vleminckx, K., Wong, E., Guger, K., Rubinfeld, B., Polakis, P., and Gumbiner, B.M. (1997). Adenomatous polyposis coli tumor suppressor protein has signaling activity in *Xenopus* laevis embryos resulting in the induction of an ectopic dorsoanterior axis. J. Cell Biol. *136*, 411–420.

von Kries, J.P., Winbeck, G., Asbrand, C., Schwarz-Romond, T., Sochnikova, N. Dell'Oro, A., Behrens, J., and Birchmeier, W. (2000). Hot spots in β-catenin for interactions with LEF-1, conductin and APC. Nat. Struct. Biol. *7*, 800–807.

Wodarz, A., and Nusse, R. (1998). Mechanisms of Wnt signaling in development. Annu. Rev. Cell Dev. Biol. *14*, 59–88.

Zhurinsky, J., Shtutman, M. and Ben-Ze'ev, A. (2000). Plakoglobin and β-catenin: protein interactions, regulation and biological roles. J. Cell Sci. *113*, 3127–3139.

Protein Data Bank ID Code

The coordinates of the β-catenin/XTcf3-CBD structure have been deposited in the Protein Data Bank with the ID code 1G3J.